UNIVERSITYOF BIRMINGHAM

University of Birmingham
Research at Birmingham

Dynamic-context cooperative quantum-behaved particle swarm optimization based on multilevel thresholding applied to medical image segmentation

Li, Yangyang; Jiao, Licheng; Shang, Ronghua; Stolkin, Rustam

[Link to publication on Research at Birmingham portal](#)

Accepted Manuscript

Dynamic-Context Cooperative Quantum-Behaved Particle Swarm Optimization Based on Multilevel Thresholding Applied to Medical Image Segmentation

Yangyang Li, Licheng Jiao, Ronghua Shang, Rustam Stolkin
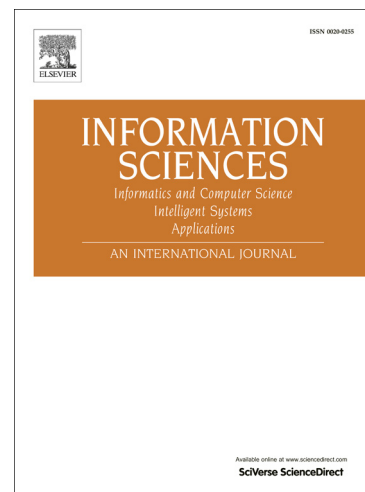
Please cite this article as: Y. Li, L. Jiao, R. Shang, R. Stolkin, Dynamic-Context Cooperative Quantum-Behaved Particle Swarm Optimization Based on Multilevel Thresholding Applied to Medical Image Segmentation, *Information Sciences* (2014), doi: http://dx.doi.org/10.1016/j.ins.2014.10.005

Dynamic-Context Cooperative Quantum-Behaved Particle Swarm Optimization Based on Multilevel Thresholding Applied to Medical Image Segmentation

Yangyang Li[a]*, Licheng Jiao[a], Ronghua Shang[a] and Rustam Stolkin[b]

[a]Key Laboratory of Intelligent Perception and Image Understanding of Ministry of Education of China, International Research Center for Intelligent Perception and Computation, Xidian University, Xi'an 710071, China

[b]School of Mechanical Engineering, University of Birmingham, Birmingham B15 2TT, UK

*yyli@xidian.edu.cn

Abstract: This paper proposes a dynamic-context cooperative quantum-behaved particle swarm optimization algorithm. The proposed algorithm incorporates a new method for dynamically updating the context vector each time it completes a cooperation operation with other particles. We first explain how this leads to enhanced search ability and improved optimization over previous methods, and demonstrate this empirically with comparative experiments using benchmark test functions. We then demonstrate a practical application of the proposed method, by showing how it can be applied to optimize the parameters for Otsu image segmentation for processing medical images. Comparative experimental results show that the proposed method outperforms other state-of-the-art methods from the literature.

1. Introduction

1.1 Background

Medical imaging, in the form of X-ray radiography, transformed medicine with its introduction more than a century ago. The availability of powerful computing resources, as well as advances in physics and other technologies, saw the rapid proliferation of additional methods over the past few decades, including CT, MRI and

ultrasound imaging. This in turn has led to a rapidly increasing demand for powerful and computationally efficient numerical methods for processing ever increasing numbers of such images to improve their clarity and automatically extract salient information to assist medical professionals.

Effective medical image processing methods are needed to help the doctor to gain more useful information, with greater accuracy, in shorter amounts of time. A particularly important capability is image segmentation, [44]. Segmentation is the process of partitioning an image into a set of non-intersecting regions, such that each region is homogeneous but the union of no two adjacent regions is homogeneous. This is a fundamental problem in Computer Vision, and a number of methods have been proposed for solving it, [43],[38]. In medical imaging, the goal of segmentation is to simplify and/or change the representation of an image, to make it more meaningful and easier to analyze.

To define a dissimilarity measure between neighboring regions, we must first define an appropriate feature space. Features like grayscale [6], color [15], texture [59], local statistical characteristics [8], and spectrum characteristics, [37], are useful for segmentation purposes, and can be extracted from an image region. Popular medical image segmentation methods can broadly be divided into region growing algorithms, [45], and edge or boundary detection methods, [52].

Thresholding is the simplest and most commonly used parallel detecting method for segmentation [49]. Thresholding is often used as a preprocessing step, followed by other post-processing methods (e.g. [23], [3], [19]). It is also commonly used for skin or bone segmentation in CT images, [5].

Single threshold segmentation can separate an object from the background, whereas multi-threshold methods, e.g. [17], are often needed to distinguish multiple salient objects. For binary segmentation of grayscale images, a common approach is to represent objects or salient regions as distributions of pixel grey-levels (Gaussian distributions or histograms are commonly employed), and use the minimum value of the intersection between the two distribution peaks to set the threshold, [6]. Alternatively, a variety of objects can be distinguished by setting multiple thresholds

at each local minima over a distribution curve of all image pixels, [17].

A shortcoming of these simple approaches is that they may not be suitable for multichannel images or images with similar characteristic values. Additionally, they may fail when the distribution of pixels for a salient object or image region is mult-modal. In addition, such methods fail to exploit spatial information contained in images, [4], [18], which can be combined with other kinds of imaging parameters [25], [63], and a-priori knowledge, [53]. Thresholding is also sensitive to uneven noise and grayscale distribution, for example different thresholds might be necessary at different locations in the same image. To overcome these difficulties, many scholars have proposed improvement methods, such as transition region determination, [62], variable thresholding with pixel spatial location information, [40], and unsupervised connectivity-based thresholding segmentation, [31].

Selecting the appropriate threshold is a difficult problem for images containing multiple objects or segmentation categories, and has received considerable attention from researchers in recent years. Pun, [46], proposed threshold selection based on a maximum entropy principle which is now recognized as one of the most important automatic threshold selection methods. This approach attempts to divide an image's greyscale histogram into multiple classes, in a way which maximises the expected information. Kapur et al. further developed this method [26]. Sahoo et al. proposed replacing the general entropy with Renyi entropy [48]. Jui-Cheng Yen et al. proposed an alternative threshold selection method, based on the max-relativity principle [60], to replace the general maximum entropy principle.

The Otsu method [42] is a nonparametric and unsupervised method of automatic threshold selection for image segmentation. In Otsu, an optimal threshold is selected according to a discriminant criterion. The procedure is very simple, however the computation time grows exponentially with the number of thresholds due to its exhaustive searching strategy, which would limit the multiple thresholding applications [17]. To overcome this problem, researchers have attempted to replace the exhaustive search strategy of the original Otsu method with more advanced numerical optimization methods, [21], [61], and there is an emerging interest in the

use of partical swarm optimization (PSO) methods to tackle this problem, [56].

1.2 Particle swarm optimisation

The past 20 years has seen a growing interest in the use of particle swarm optimization (PSO) methods, for solving difficult numerical optimization problems, especially those involving large search spaces, discontinuous or un-differentiable surfaces, and other problems. PSO is useful because it is simple to understand and program, it does not rely on any assumptions about the underlying problem space, and it uses only a small number of parameters. Since 2003, many improved swarm intelligence algorithms have been proposed, [64], [10]. However, like other intelligent heuristic-based methods, PSO cannot guarantee globally optimal convergence, and can easily become distracted by local optima. In [32], we proposed a cooperative quantum-behaved particle swarm optimization algorithm for numerical optimization (CQPSO), which addresses these problems by making use of quantum uncertainty and cooperation mechanisms. In this paper we improve the performance of our previous work, [32], by proposing a new method for dynamically updating the context vector at each iteration, and we also show how to combine this approach with the Otsu segmentation method to deliver high performance processing of medical images.

The PSO literature can roughly be divided into work which addresses: the improvement of the algorithm; algorithm analysis; and applications of PSO algorithms. Many attempts have been made to improve the performance of PSO. The use of binary system particle swarm optimization, for optimizing the structure of neural networks, was proposed by Kennedy and Eberhart in 1997, [29]. Shi and Eberhart introduced an inertia factor, w, into PSO and improved the convergence property, [50]. An extension of this work employed fuzzy systems to nonlinearly change the inertia weight during optimization, [51]. Clerc (1999) introduced the Contraction-Expansion factor into evolution algorithms to guarantee the convergence of the algorithm, [33], while relaxing the speed limit. In 1998 and 1999, [1, 2], the concept of selection and crossover was introduced into PSO by Angeline. This process involves comparing fitness values to eliminate less fit particles while a new

population is formed by selecting the more fit particles from the parent population and the offspring population. Lovbjerg et al. made a further study of PSO with selection and crossover, proposing a successful form of crossover operation, [35].

Population diversity is particularly important for improving the global convergence of PSO algorithms. The concept of "special scope" was introduced into the standard PSO algorithm by Suganthan, [54]. In order to enhance the population diversity, Kennedy, [27], introduced neighborhood topology to PSO, and also introduced "social beliefs" to enhance information exchange between neighborhoods. In 2001, Lovbjerg and his colleagues introduced the concept of sub-populations of the genetic algorithm and introduced a reproduction operator into the PSO algorithm, [54]. In 2004, Kennedy demonstrated improved performance of the PSO algorithm by employing ring topology, and made the particles move according to normally distributed random perturbations, [28]. Later in 2004, Krohling, [30], replaced the change of acceleration factor by a normal distribution, showing an improvement in the global search ability of the particle swarm.

PSO algorithms are not guaranteed to converge on global optima, and may sometimes even fail to find local optima. In 2004, Sun Jun et al. proposed a new PSO model inspired by quantum mechanics to address some of these drawbacks, [55]. This new PSO model is based on the Delta potential well, and models the particles as having quantum behaviors. Our recent work, [32], extended this by combining quantum uncertainty with cooperation mechanisms.

1.3 Quantum PSO methods

Quantum-behaved PSO algorithms are more efficient than conventional PSO. The quantum system is not a simple linear system, but a complex nonlinear system, and follows the superposition principle of states. It therefore encodes more states than the simple conventional linear system. In the quantum system, the trajectory of the particles is non-deterministic. The particles can appear anywhere in the feasible region, even a position far away from the current position, according to the probability density function. Positions that are different from the current particle's

position, may have a better fitness value than the best objective function call of the current population of particles. Therefore, incorporating the stochastic quantum behaviour enables the particles to better explore the search space and helps avoid local minima convergence.

In 2008, Leandro dos Santos Coelho [11] proposed an improved quantum-behaved swarm optimization with chaotic mutation operator. Soon after, from 2009 to 2014, more improved quantum-behaved swarm optimization methods were proposed, e.g. [36, 57, 32, 24, 13, 39, 14, 47, 22]. Y.G. Fu et al. combined differential evolution with the QPSO algorithm (DEQPSO) in an attempt to further enhance the performance of both algorithms [16]. Ch et al. investigated the accuracy of the hybrid SVM-QPSO model [7]. To further improve robustness against local minima, an improved PSO algorithm based on combining simulated annealing (SA), co-evolution theory, quantum behavior theory and diversity-guided mutation strategy (MSCQPSO) was proposed in [34].

Accompanying these advances in performance, there have been increasing numbers of applications of QPSO appearing in the literature, including image segmentation, [56], orthogonal MIMO radar, [33], and other applications, [12, 41, 47, 58].

1.4 Contributions of this work

Our work extends previous quantum PSO methods [17,36,57] in several ways. In [17,36,57], the measurement process consists in randomly sampling only once from the wave function distribution, which leads to a loss of information. In contrast, we draw multiple samples which preserves additional information about the shape of the distribution. These multiple measurements are then combined using a cooperation procedure. Additionally, we propose a new way of dynamically updating the context vector during the cooperation procedure. Cooperation is performed successively between the context vector and each of the multiple measurement samples, and the context vector is itself updated after each such cooperation. Additionally we show how Dynamic-Context Cooperative Quantum PSO (CCQPSO) can be applied to a practical problem in medical imaging, by using it to optimize the parameters of Otsu

segmentation for dividing the pixels of medical images into multiple classes.

1.5 Structure of this paper

Section 2 explains our proposed algorithm. It introduces PSO methods, describes the extension of quantum particles, and explains the notion of context vectors and how they can be used to enhance cooperative behaviour. Section 3 presents the results of comprehensive empirical testing on benchmark data-sets, and comparisons against other state-of-the-art methods. Section 4 draws concluding remarks and makes suggestions for future work.

2. Introduction to the proposed algorithm

2.1 Particle Swarm Optimization

In the classical PSO model, the ith particle is assigned the properties of position, X_i, and velocity, V_i, and propagated using the following evolutionary equation:

$$V_i(t+1) = V_i(t) + c1*r1(t)*(P_i(t) - X_i(t)) + c2*r2(t)*(P_g(t) - X_i(t)). \quad (1)$$

In 1998, Shi [50] proposed the widely used Standard PSO, introducing the parameter ω into the equation:

$$V_i(t+1) = \omega*V_i(t) + c1*r1(t)*(P_i(t) - X_i(t)) + c2*r2(t)*(P_g(t) - X_i(t)), \quad (2)$$

where $c1$ and $c2$ are the accelerated coefficients or learning factors,. Commonly $c1 = c2 = 2$ and usually $c1 = c2 \in (0,4)$. $r1$ and $r2$ are uniformly distributed random numbers from 0 to 1. P_i is the best known position of particle i and P_g be the best known position of the entire swarm.

2.2 Quantum Particle Swarm Optimization

In PSO, particles move along deterministic paths, at speeds which are limited by the available computing resources. This limits the ability of such algorithms to find global optima, and makes them prone to local optima convergence. To overcome the limitations of these deterministic particle paths, researchers have attempted to

introduce an element of stochasticity into particle paths, making an analogy with the probabilistic quantum mechanical descriptions of the motions of subatomic particles in the physics literature. Early work in this area included Jun et al., [55], in 2004.

In terms of classical mechanics, a particle's motion can be completely described by its position vector and velocity vector, which determine the trajectory of the particle. The particle moves along a deterministic trajectory in Newtonian mechanics, but this is not the case in quantum mechanics. In the quantum world, the position and the velocity of a particle can never both be determined simultaneously, according to Heisenburg's uncertainty principle, [20]. Instead, the particle state must be described probabilistically.

The wave function, $\psi(\vec{x},t)$, probability density function, $\left|\psi(\vec{x},t)\right|^2$ and, within a 3D space, $\left|\psi(\vec{x},t)\right|^2 dxdydz$, represents the probability of a particle being discovered within the volume element, $dxdydz$ at time t. The wave function is obtained by solving the Schrodinger equations, based on a Delta potential well:

$$\begin{cases} V(X) = -\gamma\delta(X-p) = -\gamma(y) \\ \hat{H} = -\dfrac{\hbar^2}{2m}\nabla^2 + V(X) \\ -i\hbar\dfrac{\partial}{\partial t}\psi(X,t) = \hat{H}\psi(X,t) \end{cases} \tag{3}$$

where point P is the center of the well. Solving the Schrodinger equations, [55], yields the wave function:

$$\psi(y) = \frac{1}{\sqrt{L}}e^{-|y|/L}, \tag{4}$$

where, $L = \dfrac{\hbar^2}{m\gamma}$, $y = X - p$, $V(x)$ is the potential well function. $\hat{H}$ is the Hamiltonian operator. ∇^2 is the Laplace operator. This gives the probability density function as:

$$Q(y) = \left|\psi(y)\right|^2 = \frac{1}{L}e^{-2|y|/L}. \tag{5}$$

The above functions describe the location of a particle probabilistically, analogously to quantum theory. However, to evaluate a fitness function (i.e. converting from the search space to the solution space) for numerical optimisation, we need to use an exact, explicit particle position. Converting from a density function to an explicit position is achieved by using a Monte Carlo method to simulate a position "measurement". The procedure of measurement simulation is described as follows.

Let s be a uniformly distributed random number:

$$s = \frac{1}{L} rand(0,1) = \frac{1}{L} u .$$
(6)

Substituting s for $|\psi(y)|^2$, we obtain:

$$s = \frac{1}{L} e^{-2|y|/L} ,$$
(7)

and hence $u = e^{-2|y|/L}$,
(8)

yielding $y = \pm \frac{L}{2} \ln(1/u)$.
(9)

This finally gives the estimated position X_{id} of the ith particle in the d-dimensional search space (where p_{id} is the attractor of the ith particle) as:

$$X_{id} = p_{id} \pm \frac{L}{2} \ln(1/u) .$$
(10)

In [55], L is evaluated with the current particle position X_{id} and attractor p_{id}:

$$L = 2 * \alpha * |p_{id} - X_{id}| .$$
(11)

Finally, the particle position is updated based on the delta potential well model:

$$X_{id}(t+1) = p_{id} \pm \alpha * |p_{id} - X_{id}(t)| * ln(1/u) ,$$
(12)

where α, known as the "expansion factor", is a unique parameter of the quantum-behaved particle swarm optimization algorithm based on the Delta potential well, and is generated from a uniformly distributed random function in the interval [0, 1].

2.3 Cooperative quantum-behaved particle swarm optimization algorithm (CQPSO)

J. Sun et al. incorporated a context vector in cooperative quantum-behaved particle

swarm optimization (sunCQPSO), [17]. The context vector was designed to evaluate each dimension of a particle appropriately in the processing of cooperation. In sunCQPSO, the globally optimal particle in each generation is assigned as the context vector. In contrast, at each generation, for each particle we use the Monte Carlo measurement procedure to sample multiple measurements, [32]. In [32], we showed how to set the best of these samples to be a local context vector for that particle.

Search algorithms which include stochasticity (including quantum particle swarm optimization and genetic algorithms) suffer from the "curse of dimensionality", which refers to the phenomenon of scaling problems with high dimensional data. Every dimension of a particle will affect its overall fitness. Therefore, some particles will be associated with low fitness, even if some of their dimension values lie very close to the corresponding dimensions of the globally optimal solution. This is why the cooperation operation is important, as it enables information from the "good" dimensions to be preserved within the particle swarm and can prevent potentially useful information from being unnecessarily discarded. By performing cooperation one dimension at a time, we are able to evaluate each dimension respectively, and save the most useful information to accelerate convergence. We now describe how our proposed method extends the notion of cooperation in quantum PSO, by generating new individuals by performing cooperation between multiple Monte Carlo measurements for each particle.

In general, our proposed method could be used to cooperate between an arbitrary number of measurement samples. The greater the number of such observations, the greater will be the utilization efficiency of the quantum-induced uncertainty, and the faster the convergence rate. However, the total processing time grows linearly. For proof of principle, we will here explain the algorithm assuming that the wave function is sampled by the measurement procedure to generate five new individuals: $X_{l1}(x_{11},x_{12},...,x_{1D},)$, $X_{l2}(x_{21},x_{22},...,x_{2D})$, $X_{l3}(x_{31},x_{32},...,x_{3D})$, $X_{l4}(x_{41},x_{42},...,x_{4D})$ and $X_{l5}(x_{51},x_{52},...,x_{5D})$, then we compute:

$$mbest = (\frac{1}{M}\sum_{i=1}^{M} P_{i1}, \frac{1}{M}\sum_{i=1}^{M} P_{i2}, ..., \frac{1}{M}\sum_{i=1}^{M} P_{id}), \qquad (13)$$

$$P_i(t+1) = \varphi * P_i(t) + (1-\varphi)*P_g, \qquad (14)$$

$$X_i(t+1) = P_i(t+1) \pm \alpha * |mbest - X_i(t)| * \ln(1/u), \qquad (15)$$

where $mbest$ is the mean position of the whole particle swarm. $P_i(t+1)$ is the new particle, which combines information from $P_i(t)$ (the "personal best" position achieved by the ith particle throughout its history) and P_g (the globally best particle over the whole population). M is the population size, and φ and u are uniformly distributed random numbers from 0 to 1. α is known as the Creativity Coefficient, and is the only parameter which needs to be specified.

2.4 Dynamic-Context Cooperative Quantum-behaved Particle Swarm Optimization Algorithm

The previous section showed how to sample multiple measurements, and combine these through cooperation. In our previous work, [32], we selected the best of these measurement vectors and set it as the context vector. This context vector then remained constant throughout the cooperation procedure. In contrast, we now explain how to continually update the context vector dynamically during cooperation, to take account of any new information obtained at each successive stage of the cooperation process. This dynamic update procedure makes best use of new information and so accelerates the rate of convergence. After each particle evaluation is completed, that particle will update its own context vector according to the procedure shown in Fig. 1. In this paper, for proof of principle, each particle generates five particles through five simulated measurements as mentioned above. We therefore obtain five individuals and then select the best individual X_{i_B} according to its fitness value among five individual. Then we assign X_{i_B} as the current local context vector for the ith particle P_i. This context vector is then cooperated with the remaining four individuals obtained from the measurement process. For each dimension of the context vector, the

corresponding dimension of each of the other four individuals is substituted, and tested to see if the replacement dimension improves the fitness value. If it does, the substitute value is adopted and the resulting vector is used to replace the context vector. This procedure is repeated until all dimensions of all five measurement vectors have been evaluated, and the best permutation is selected to form a new particle for the new generation. This procedure is shown in figure 1.

Procedure:
Initialize population: Xi
$Pbest=Xi$
$Gbest$=best $Pbest$
if $t<Gmax$
for each particle
generate five particles using Eq.(13) to Eq.(15)
select $Xi=$ X_{i_B}
$Xc=Xlj$
for each particle Xk
$f=f(Xc)$
for each dimension j
if $f(Xc(j,Xkj))<f$
$Xij= Xkj$
endif
$Xc=$ X_{i_B}
end
$Xc= Xi$
end
if $f(Xi)<f(Pbesti)$
$Pbesti=Xi$
endif
if $f(Pbesti)<f(Gbest)$
G$best=Pbesti$
endif
end

Fig. 1. Pseudo-code procedure for Dynamic-Context Cooperative Quantum-behaved particle swarm optimization (CCQPSO).

3. Experimental results

3.1 Experiments using benchmark optimization functions

To investigate the performance of our proposed Dynamic Context Cooperative

Quantum-behaved particle swarm optimization (CCQPSO) algorithm, we have tested CCQPSO using five benchmark test functions. Table 1 lists the basic characteristics of these test functions. These benchmark functions are all minimization problems with zero global minimum values. For each function, we compare the performance of CCQPSO against: quantum-behaved particle swarm optimization algorithm with weighted mean best position (WQPSO) [58]; the cooperative quantum particle swarm algorithm presented by J-Sun et al. (sunCQPSO) [17]; and our previously proposed cooperative quantum-behaved particle swarm optimization (CQPSO) [32].

For CCQPSO, the size of the initial population is 20 and we set the parameter *measurements* $= 5$. We performed 50 trial runs for each algorithm on each benchmark function, and recorded the mean best fitness and standard deviation over the 50 trials. For sunCQPSO and CQPSO, relaxation factor α decreases linearly from 1.0 to 0.5. All trials were performed using a 2.33GHz Pentium IV PC with 2G RAM running Matlab implementations of the algorithms.

The results are shown in Table 2 and Table 3, where M is the size of population, D is the number of dimensions and Gmax is the maximum allowed number of generations.

Table 1 Basic characteristic of test functions

The functions	Expression	Initialization interval	Maximal area
Sphere function $f1$	$f1(x) = \sum_{i=1}^{n} x_i^2$	(-50,100)	100
Rosenbrock function $f2$	$f2(x) = \sum_{i=1}^{n}(100(x_{i+1} - x_i^2) + (x_i - 1)^2)$	(15,300)	100
Rastrigin function $f3$	$f3(x) = \sum_{i=1}^{n}(x_i^2 - 10\cos(2\pi x_i) + 10)$	(2.56,5.12)	10
Griewank function $f4$	$f4(x) = \frac{1}{4000}\sum_{i=1}^{n} x_i^2 - \prod_{i=1}^{n}\cos(\frac{x_i}{\sqrt{i}}) + 1$	(-300,600)	600
De Jong's function $f5$	$f5(x) = \sum_{i=1}^{n} i x_i^4$	(-30,100)	100

From Table 2 and Table 3 it can be seen that our proposed CCQPSO method significantly outperforms all the other comparison methods on all five benchmark functions and the performance variance of the proposed method is also small, suggesting stability.

Table 2 Test function comparison between WQPSO and sunQPSO

f	M	D	Gmax	WQPSO		sunCQPSO	
				Mean Min	St.Var	Mean Min	St.Var
$f1$	20	20	1500	2.4267E-38	5.8824E-38	4.946880e-317	0.0000E+00
		30	2000	6.9402E-32	1.2879E-31	0.0000E+00	0.0000E+00
		100	3000	4.2014E-11	4.0006E-11	2.4209E-218	0.0000E+00
$f2$	20	20	1500	4.4948E+01	5.8837E+01	3.7499E+01	4.8401E+01
		30	2000	7.6625E+01	1.0193E+02	5.5191E+01	6.4979E+01
		100	3000	2.4832E+02	1.9868E+02	8.4586E+01	4.2951E+01
$f3$	20	20	1500	1.2945E+01	4.0725E+00	0.0000E+00	0.0000E+00
		30	2000	2.4259E+01	7.9174E+00	5.9698E-02	2.3869E-01
		100	3000	2.1121E+02	3.5535E+01	9.1352E+00	7.0400E+00
$f4$	20	20	1500	2.4863E-02	2.3981E-02	4.2273E-02	4.3296E-02
		30	2000	9.0994E-03	1.2641E-02	6.1817E-02	6.9100E-02
		100	3000	4.4359E-03	9.0706E-03	4.4409E-18	2.1977E-17
$f5$	20	20	1500	2.4224E-50	1.5425E-49	0.0000E+00	0.0000E+00
		30	2000	1.5686E-40	5.9721E-40	0.0000E+00	0.0000E+00
		100	3000	7.7518E-11	7.8925E-11	5.3694E-285	0.0000E+00

Table 3 Test function comparison between CQPSO and CCQPSO

f	M	D	Gmax	CQPSO		CCQPSO	
				Mean Min	St.Var	Mean Min	St.Var
$f1$	20	20	1500	0.0000E+00	0.0000E+00	**0.0000E+00**	**0.0000E+00**
		30	2000	4.4466E-323	0.0000E+00	**0.0000E+00**	**0.0000E+00**
		100	3000	3.6129E-98	2.5448E-97	**0.0000E+00**	**0.0000E+00**
$f2$	20	20	1500	2.9140E+01	5.6023E+01	**1.8557E+00**	**2.5443E+00**
		30	2000	2.9660E+01	4.6534E+01	**1.1051E+00**	**1.1660E+00**
		100	3000	1.4697E+02	9.3562E+01	**2.0581E+01**	**1.4751E+01**
$f3$	20	20	1500	1.2198E+01	6.4537E+00	**5.9698E+00**	**3.9798E+00**
		30	2000	1.8049E+01	6.3279E+00	**1.1343E+01**	**3.8918E+00**
		100	3000	1.1293E+02	1.7379E+01	**4.7161E+01**	**6.5471E+00**
$f4$	20	20	1500	1.9176E-02	1.6191E-02	**1.3727E-02**	**2.0671E-02**
		30	2000	1.0279E-02	1.5108E-02	**0.0000E+00**	**0.0000E+00**
		100	3000	2.6110E-03	5.1311E-03	**0.0000E+00**	**0.0000E+00**
$f5$	20	20	1500	0.0000E+00	0.0000E+00	**0.0000E+00**	**0.0000E+00**
		30	2000	0.0000E+00	0.0000E+00	**0.0000E+00**	**0.0000E+00**
		100	3000	3.7938E-104	1.4349E-103	**0.0000E+00**	**0.0000E+00**

Figure 2 plots log fitness of the measurement vectors against numbers of generations for CCQPSO, CQPSO and sun CQPSO, for the "Sphere" benchmark test function, $f1$. Clearly the proposed CCQPSO significantly outperforms the other

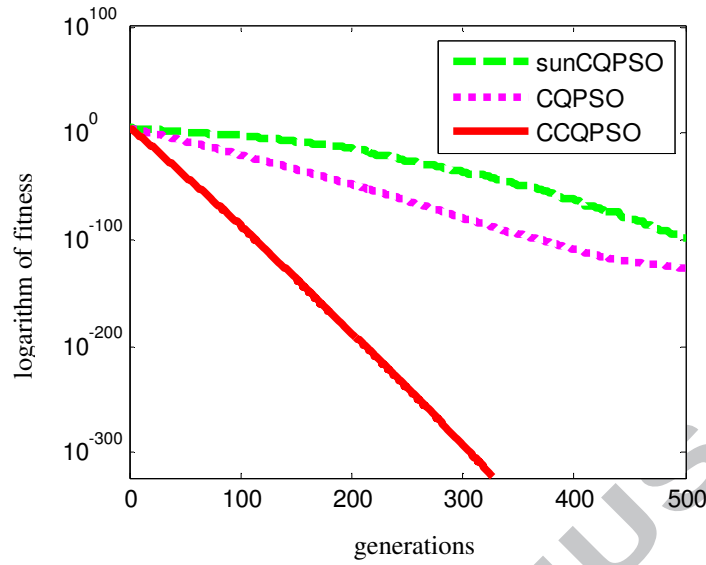methods, demonstrating significantly more rapid convergence.

Fig. 2. Comparison of convergence of "measurement" values for Sphere function $f1$. Note, we only compare against sunCQPSO and CQPSO, because WQPSO does not use "context" vector.

In order to test the significance between CCQPSO and other comparison algorithms, the Student's t Test was used. It can be calculated by the follow formula:

$$t = \frac{\overline{X_1} - \overline{X_2}}{\sqrt{\dfrac{(n_1-1)S_1^2 + (n_2-1)S_2^2}{n_1+n_2-2}\left(\dfrac{1}{n_1}+\dfrac{1}{n_2}\right)}} \quad , \tag{16}$$

where, n_1, n_2 is the sample number of the two the sample sets, $\overline{X_1}, \overline{X_2}$ is their average value, and S_1^2, S_2^2 is their variance. Because n_1 and n_2 are equal, and we set $n = n_1 = n_2$, the formula can be simplified to:

$$t = \frac{\overline{X_1} - \overline{X_2}}{\sqrt{\dfrac{S_1^2 + S_2^2}{n}}} \quad . \tag{17}$$

The result of the Student's t Test is shown in Table 4. The negative value means that the result of our algorithm is better. From the table we can see that our algorithm is better than WQPSO on all the test functions. And our algorithm is better than sunCQPSO on $f2$ and $f4$. On $f3$, sunCQPSO is better than CCQPSO, but on $f1$(100 dimension), $f2$-$f4$, and $f5$(100 dimension) our algorithm is better than CQPSO. Therefore, the advantages of our proposed CCQPSO algorithm become more obvious

with increasing numbers of dimensions.

Table 4. Results of Student's *t* Test between CCQPSO and comparison algorithms

f	D	CCQPSO-WQPSO	CCQPSO-sunCQPSO	CCQPSO-CQPSO
$f1$	20	-7E-19	0	0
	30	-1.4E-15	0	0
	100	-4.6E-05	0	-5E-49
$f2$	20	-38.4992	-34.9534	-24.9535
	30	-52.0597	-46.5459	-28.9352
	100	-109.099	-58.9391	-84.9774
$f3$	20	-17.2059	20.94743	-13.4967
	30	-26.3993	38.72308	-14.7794
	100	-176.972	72.27895	-94.0588
$f4$	20	-0.36967	-0.79064	-0.19957
	30	-0.56653	-1.64614	-0.58539
	100	-0.32603	-6.6E-09	-0.25515
$f5$	20	-4.3E-25	0	0
	30	-4.5E-20	0	0
	100	-6.1E-05	0	-7E-52

3.2 Medical Image segmentation

To demonstrate an application of the proposed CCQPSO algorithm, we now demonstrate its performance on a medical imaging problem. We use CCQPSO to optimize the parameters for Otsu image segmentation of six different CT images showing cross-sections through a human stomach cavity. Each image is 512*512 pixels. The algorithm is tasked with segmenting each image pixel into one of three classes, based on grey level intensity, such that the three classes are as distinct as possible from each other. Again, we compare the proposed CCQPSO algorithm against CQPSO [32] and sunCQPSO [17].

During all trials, the algorithm parameter are set as follows. For sunQPSO [17], CQPSO [32] and CCQPSO, the populations are all set to 20, and relaxation factor α decreases linearly from 1.0 to 0.5. For CQPSO and CCQPSO, the number of measurements is set to 5, and the iterations argument is 100. We performed 10 trial runs for every instance and recorded mean optimal threshold, mean inter-class

variance and standard deviation. The simulation has been carried out on a 2.33GHz Pentium IV PC with 2G RAM using algorithm implementations in Matlab.

**Table 5** Segmentation data of the three algorithms on stomach CT images 200.1 and 200.2

	200.1			200.2		
	Optimal Threshold	Inter-Class Variance	St.Var	Optimal Threshold	Inter-Class Variance	St.Var
sunCQPSO	39,193	5236.6340	4.0600E+01	59,165	5204.1790	5.7500E+01
CQPSO	43,171	5251.2720	1.1972E+02	72,208	5224.1460	4.8833E+01
CCQPSO	62,176	5315.6780	0.0000E+00	62,176	5275.4370	9.5900E-13

Table 6 Segmentation data of the three algorithms on stomach CT images 200.10 and 200.86

	201.10			201.86		
	Optimal Threshold	Inter-Class Variance	St.Var	Optimal Threshold	Inter-Class Variance	St.Var
sunCQPSO	44,138	3956.0970	2.5400E+01	45,119	4740.0140	2.4300E+01
CQPSO	73,209	3963.1870	2.8674E+01	67,159	4730.3980	1.3452E+01
CCQPSO	56,146	3990.3230	4.7900E-13	55,139	4765.4210	9.5900E-13

**Table 7** Segmentation data of the three algorithms on stomach CT images 200.14 and 200.29

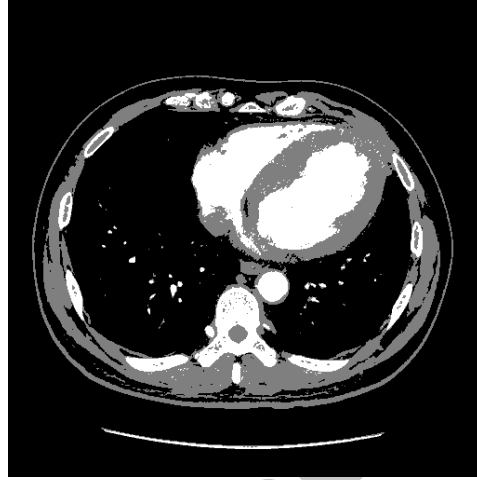|	200.14			201.29		
	Optimal Threshold	Inter-Class Variance	St.Var	Optimal Threshold	Inter-Class Variance	St.Var
sunCQPSO	58,176	4.5421E+03	6.7260E+01	68,201	3.9453E+03	6.2061E+01
CQPSO	73,154	4.5453E+03	4.4676E+01	83,212	3.9497E+03	1.9377E+01
CCQPSO	62,172	4.5999E+03	9.5869E-13	67,182	3.9835E+03	9.5869E-13
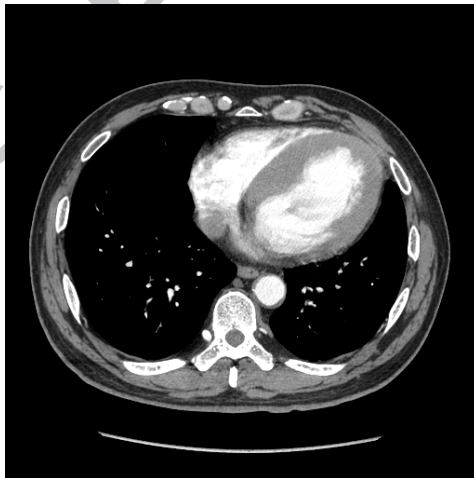
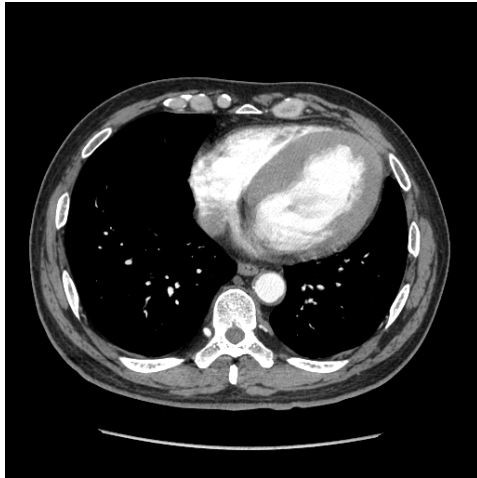(a) Original image   (b) sunCQPSO
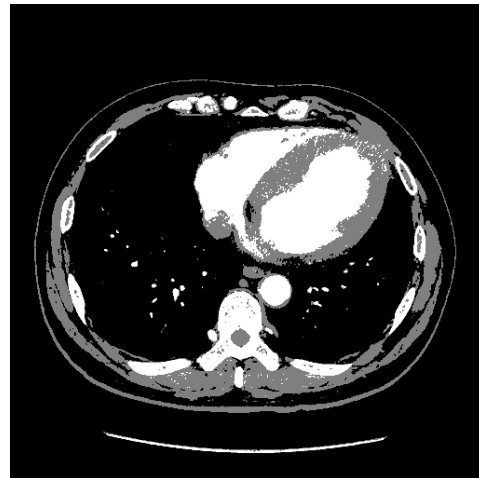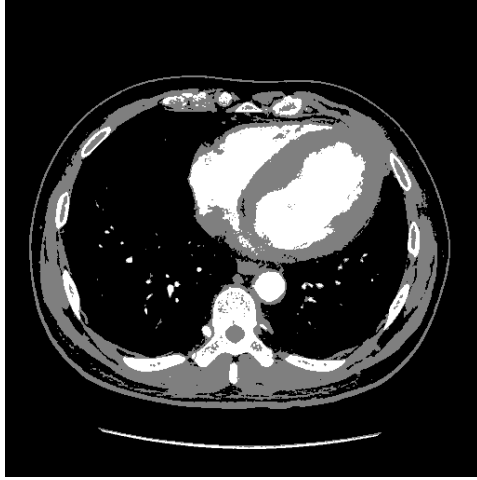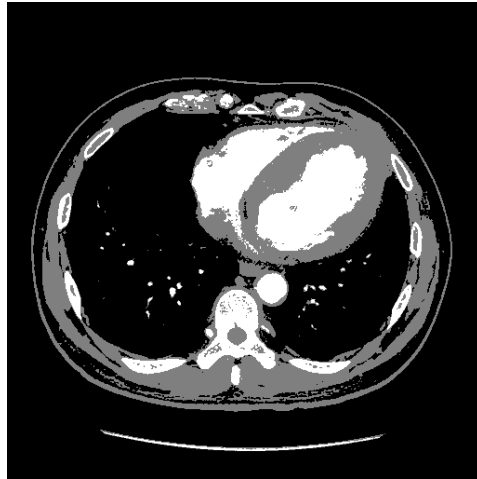
(c) CQPSO

(d) CCQPSO

Fig. 3. Segmentation results of stomach image "CT 200.1". The three classes are denoted by white, grey and black respectively.
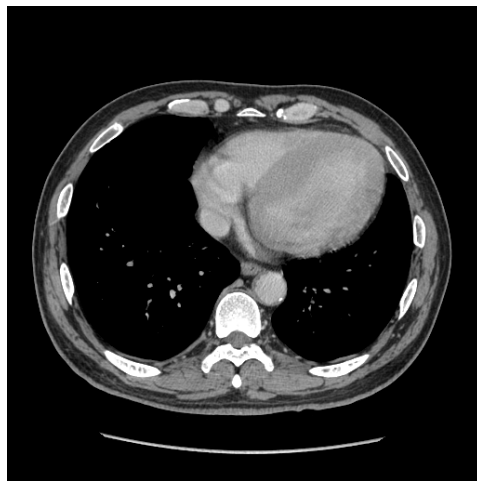

(a) Original image

(b) sunCQPSO

(c) CQPSO　　　　　　　　　　　(d) CCQPSO

Fig. 4. Segmentation results of stomach image "CT 200.2". The three classes are denoted by white, grey and black respectively.
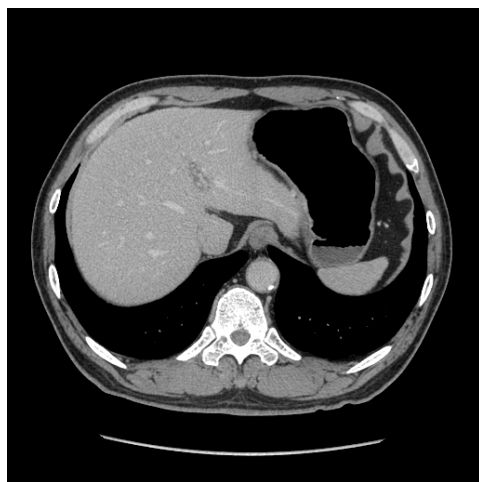

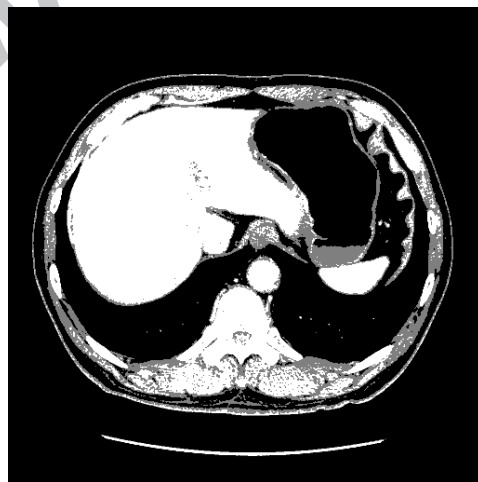(a) Original image　　　　　　　　　(b) sunCQPSO

(c) CQPSO   (d) CCQPSO
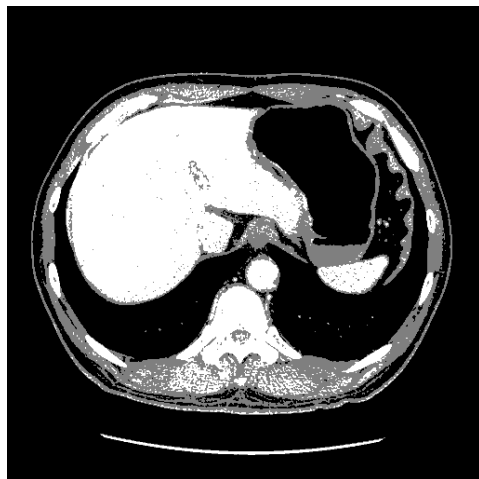
Fig. 5. Segmentation results of stomach image "CT 200.10". The three classes are denoted by white, grey and black respectively.

(a) Original image   (b) sunCQPSO

(c) CQPSO   (d) CCQPSO

Fig. 6. Segmentation results of stomach image "CT 200.86". The three classes are denoted by white, grey and black respectively.

(a) Original image   (b) sunCQPSO

(c) CQPSO   (d) CCQPSO

Fig. 7. Segmentation results of stomach image "CT 200.14". The three classes are denoted by white, grey and black respectively.

(a) Original image   (b) sunCQPSO
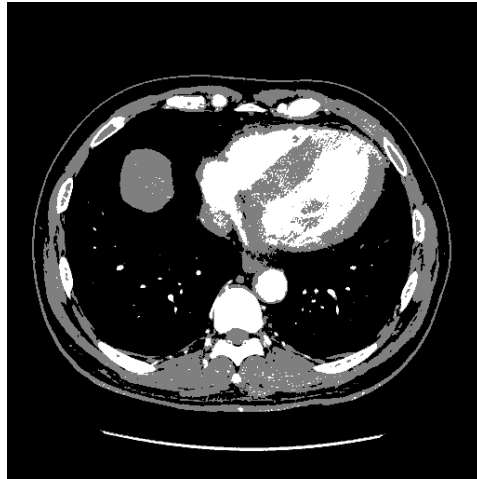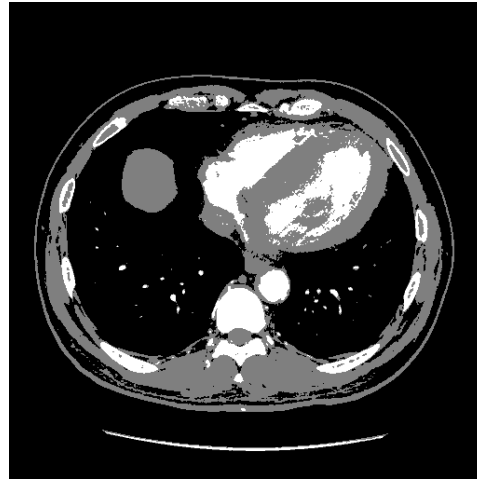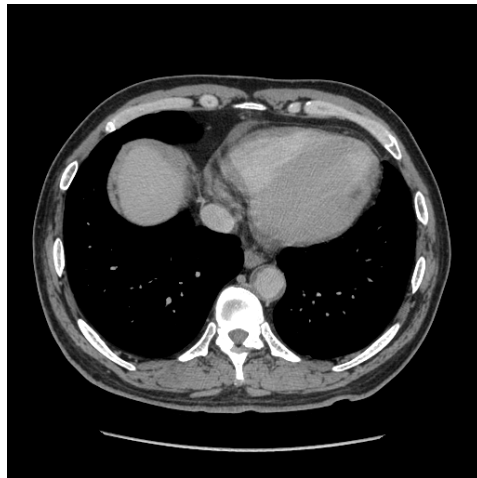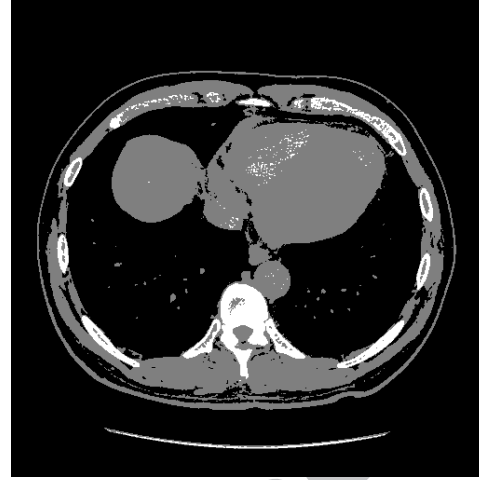
(c) CQPSO   (d) CCQPSO

Fig. 8. Segmentation results of stomach image "CT 200.29". The three classes are denoted by white, grey and black respectively.

It can be seen from Tables 5, 6 and 7 that, image segmentation using CCQPSO produces better results in terms of variance between classes. According to the evaluation criteria of the Otsu method, the greater the value of variance between clusters the better the segmentation result is expected to be. Although the numerical results show that the proposed CCQPSO method has clustered pixels into classes that are more distinct than the comparison methods, the differences in the quality of the resulting segmented images are not obvious to the human eye.

4. Conclusion

This paper has presented a new Dynamic Context Cooperative Quantum-behaved particle swarm optimization (CCQPSO) algorithm. The aim of this method is to improve the performance of the cooperative quantum-behaved particle swarm optimization (CQPSO) algorithm by better exploiting contextual information. We have shown how context variables can be continuously and dynamically updated when evaluating different individual dimension components, during the cooperation procedure, thus making the best possible use of any new information, as soon as it becomes available to the system.

Empirical testing, on a number of different benchmark test functions, shows that CCQPSO significantly outperforms three other state of the art methods, accelerating convergence and reducing final errors. We have also shown how CCQPSO can be used to optimize the parameters of Otsu image segmentation, and we have demonstrated this method on a number of example medical images. Numerical results suggest that CCQPSO outperforms the comparison methods for image segmentation, although the resulting images, output by all three compared methods, appear visually similar to the human eye. We suggest that a reason for this is that the image characteristics, segmentation method to be optimized, and number of classes to be clustered, all conspire to provide a relatively simple optimization problem, where less sophisticated methods can still show nearly as good performance as complex methods. In future work, we hope to provide more obvious demonstrations of the advantages of CCQPSO by applying it to more complex kinds of segmentation problems on more difficult images.

5. Acknowledgments

References

[1] P. J. Angeline, Using selection to improve particle swarm optimization, Pro. of the IEEE International Conference on Evolutionary Computation. Anchorage, Alaska, 1998, pp: 84-89.

[2] P. J. Angeline, Evolutionary optimization versus particle swarm optimization philosophy and performance difference, Evolutionary Programming VII, Lecture Notes in Computer Science 1447, 1998, Springer, pp: 601-610.

[3] S. Bag, P. Bhowmick, P. Behera, et al. Robust binarization of degraded documents using adaptive-cum-interpolative thresholding in a multi-scale framework. Image Information Processing (ICIIP), 2011 International Conference on, Publication Year: 2011, Page(s): 1 - 6.

[4] J. Besag, On the statistical analysis of dirty pictures, Journal of the Royal Statistical Society, 1986, 48(3): 259-302.

[5] M. Bomans, K.-H. Hohne, et al. 3-D segmentation of MR images of the head for 3-D display. Medical Imaging, IEEE Transactions on, 1990, 9(2): 177-183.

[6] U. Braga-Neto, J. Goutsias, Grayscale level connectivity: theory and applications, IEEE Transactions on Image Processing, 2004, 13(12): 1567-80.

[7] 33 S. Ch, N. Anand, B. K. Panigrahi, S. Mathur, Streamflow forecasting by SVM with quantum behaved particle swarm optimization, Neurocomputing, 2013, 101(4), pp: 18-23.

[8] D.-Q. Chen, L.-Z. Cheng. Spatially Adapted Total Variation Model to Remove Multiplicative Noise. IEEE Transactions on Image Processing, 2012, 21(4): 1650 - 1662

[9] M. Clerc, The swarm and queen: towards a deterministic and adaptive particle swarm optimization, Pro. of the IEEE International Conference on Evolutionary Computation. Piscataway, IEEE Press, 1999: 1951-1957.

[10] M. Clerc, Discrete particle swarm optimization. In: New optimization techniques in engineering. 2004, Springer, Berlin.

[11] L. D. S. Coelho, A quantum particle swarm optimizer with chaotic mutation operator, Chaos, Solitons & Fractals, September 2008, Vol. 37, Issue 5, pp. 1409-1418.

[12] L. D. S. Coelho and V. C. Mariani, Particle swarm approach based on quantum mechanics and harmonic oscillator potential well for economic load dispatch with valve-point effects, Energy Conversion and Manage, 2008, Vol. 49, No. 11, pp.

3080-3085.

[13] E. Davoodi, M. T. Haque, S. G. Zadeh, A hybrid Improved Quantum-behaved Particle Swarm Optimization-Simplex method (IQPSOS) to solve power system load flow problems Original Research Article,Applied Soft Computing, In Press, Uncorrected Proof, Available online 31 March 2014.

[14] S. Dey, S. Bhattacharyya, U. Maulik, Quantum inspired genetic algorithm and particle swarm optimization using chaotic map model based interference for gray level image thresholding Original Research Article, Swarm and Evolutionary Computation, Volume 15, April 2014, Pages 38-57.

[15] G. Dong , M. Xie, Color clustering and learning for image segmentation based on neural networks. IEEE Transactions on Neural Networks, 2005, 16(4):925-36.

[16] Y. G. Fu, M. Y. Ding, C. P. Zhou, Route Planning for Unmanned Aerial Vehicle (UAV) on the Sea Using Hybrid Differential Evolution and Quantum-Behaved Particle Swarm Optimization, IEEE Transactions on Systems Man Cybernetics-Systems, 2013, 43(6), pp: 1451-1465.

[17] H. Gao, W. B. Xu and J. Sun, et al, Multilevel thresholding for image segmentation through an improved quantum-behaved particle swarm algorithm, IEEE Transactions on Instrumentation and Measurement, 59 (2010), pp: 934-946.

[18] S. Geman, D. Geman. Stochastic relaxation, Gibbs distributions, and the Bayesian restoration of images. Pattern Analysis and Machine Intelligence, IEEE Transactions on, 1984, (6): 721-741.

[19] D. Gupta, R. S. Anand, et al. Enhancement of Medical Ultrasound Images Using Multiscale Discrete Shearlet Transform Based Thresholding. Electronic System Design (ISED), 2012 International Symposium on, Publication Year: 2012, Page(s): 286-290.

[20] W. Heisenberg, Über den anschaulichen Inhalt der quantentheoretischen Kinematik und Mechanik, Zeitschrift für Physik 43 (3–4): 172–198, 1927.

[21] D.-Y. Huang, C.-H. Wang. Optimal multi-level thresholding using a two-stage Otsu optimization approach. Pattern Recognition Letters, 2009, 30(3): 275-284.

[22] Y.-M. Jau, K.-L. Su, C.-J. Wu, J.-T. Jeng, Modified quantum-behaved particle

swarm optimization for parameters estimation of generalized nonlinear multi-regressions model based on Choquet integral with outliers Original Research Article, Applied Mathematics and Computation, Volume 221, 15 September 2013, Pages 282-295.

[23] B. Johnston, M. S. Atkins, B. Mackiewich, et al. Segmentation of multiple sclerosis lesions in intensity corrected multispectral MRI. IEEE Transactions on Medical Imaging, 1996, 15(2): 154 - 169.

[24] H. Kamberaj, q-Gaussian swarm quantum particle intelligence on predicting global minimum of potential energy function Original Research Article, Applied Mathematics and Computation, Volume 229, 25 February 2014, Pages 94-106.

[25] T. Kapur, et al. Enhanced spatial priors for segmentation of magnetic resonance imagery. Medical Image Computing and Computer-Assisted Interventation—MICCAI'98. Springer Berlin Heidelberg, 1998. 457-468.

[26] J. N. Kapur, P. K. Sahoo, A. K. C. Wong, A new method for gray-level picture thresholding using the entropy of the histogram, Computer Vision, Graphic and Image Processing, 1985, 29(3), pp: 273-285.

[27] J. Kennedy, Small worlds and mega-minds: effects of neighborhood topology on particle swarm performance, Proc. of the IEEE International Conference on Evolutionary Computation, IEEE Press, 1999, pp: 1931-1938.

[28] J. Kennedy, Probability and dynamics in the particle swarm, Proc. of the IEEE International Conference on Evolutionary Computation, 2004, pp: 340-347.

[29] J. Kennedy and R.C. Eberhart, A discrete version of the particle swarm algorithm, Proc. of the IEEE Conference on Systems, man and Cybernetics. Piscataway, IEEE Service Center, 1997: 4104-4109.

[30] R. A. Krohling, Gaussian swarm: a novel particle swarm optimization algorithm, Proc. of the Congress on Cybernetics and Intelligent Systems, Singapore, 1-3 December, 2004: 372-376.

[31] C. Lee, S. Hun, T. A. Ketter, M. Unser, Unsupervised connectivity-based thresholding segmentation of midsaggital brain MR images, Computers in Biologist and Medicine, 1998, 28(3), pp: 309-338.

[32] Y. Y. Li, R. R. Xiang, and L. C. Jiao, et al., An improved cooperative quantum-behaved particle swarm optimization. Soft Computing, 2012, 16: 1061-1069.

[33] H. W. Liu, G. W. Yang, G. J. Song, MIMO radar array synthesis using QPSO with normal distributed contraction-expansion factor, Procedia Engineering, 2011, 15, pp: 2449-2453.

[34] F. Liu, Z. G. Zhou, An improved QPSO algorithm and its application in the high-dimensional complex problems, Chemometrics and Intelligent Laboratory Systems, 2014, 132(15), pp: 82-90.

[35] M. Lovbjerg, T. K. Rasussen and T. Krink, Hybrid particle swarm optimizer with breeding and sub populations, Proc. of the third Genetic and Evolutionary Computation Conference, 2001.

[36] S. F. Lu, C. F. Sun, and Z. D. Lu, An improved quantum-behaved particle swarm optimization method for short-term combined economic emission hydrothermal scheduling, Energy Conversion and Management, March 2010, Vol. 51, Issue 3, pp. 561-571.

[37] U. von Luxburg, A tutorial on spectral clustering. Statistics and Computing, 2007, 17(4): 395-416.

[38] Z. Ma, , J. M. Tavares, R. N. Jorge, and T. Mascarenhas, A review of algorithms for medical image segmentation and their applications to the female pelvic cavity. Computer Methods in Biomechanics and Biomedical Engineering, 2010, 13(2): 235-246.

[39] V. C. Mariani, A. R. K. Duck, F. A. Guerra, L. D. S. Coelho, R. V. Rao, A chaotic quantum-behaved particle swarm approach applied to optimization of heat exchangers Original Research Article, Applied Thermal Engineering, Volume 42, September 2012, Pages 119-128.

[40] Y. Nakagawa, A. Rosenfeld, Some experiments on Variable thresholding, Pattern Recognition, 1979, 1 1(3), pp: 191-204.

[41] S. N. Omkar, Rahul Khandelwal, and T.V.S. Ananth, et al, Quantum behaved Particle Swarm Optimization (QPSO) for multi-objective design optimization of

composite structures, Expert Systems with Applications, October 2009, Vol. 36, Issue 8, pp. 11312-11322.

[42] N. Otsu, A threshold selection method from gray-level histogram, IEEE Tran. Systems Man Cybernet, SMC-9, pp. 62-66.

[43] N. R. Pal, S. K. Pal, A review on image segmentation techniques. Pattern recognition, 1993, 26(9): 1277-1294.

[44] D. L. Pham, C. Y. Xu, and J. L. Prince, Current methods in medical image segmentation, Annual Review of Biomedical Engineering, 2000, 2: 315-337.

[45] R. Pohle, K. D. Toennies, Segmentation of medical images using adaptive region growing. Proc. SPIE Vol. 4322, p. 1337-1346, Medical Imaging 2001: Image Processing, Milan Sonka, Kenneth M. Hanson,Eds.

[46] T. Pun, A new method for gray-level picture thresholding using the entropy of the histogram, Signal Processing, 1980, 2(3), pp: 233-237.

[47] S. L. Sabat, L. D. S. Coelho and A. Abraham, MESFET DC model parameter extraction using quantum particle swarm optimization, Microelectronics Reliability, June 2009, Vol. 49, Issue 6, pp. 660-666.

[48] P. Saboo, C. Wilkins, J. Yeager, Threshold selection using renyi's entropy, Pattern Recognition, 1997, 30(1), pp: 71-84.

[49] P. K. SahfKi, S. soltani, A. K. C. Wang, Y. C. Chen, A survey of thresholding techniques, Computer Vision, Graphics and Image Processing, 1988, 41(2), pp:233-260.

[50] Y. Shi, R.C. Eberhart, A modified particle swarm optimizer, Pro. of the IEEE International Conference on Evolutionary Computation. Piscataway, IEEE Press, 1998: 69-73.

[51] Y. Shi, R.C. Eberhart, Fuzzy adaptive particle swarm optimization, Proc. of Congress on Evolutionary Computation, Seoul, Korea, IEEE Service Center, 2001, pp:101-106.

[52] K. Somkantha, N. Theera-Umpon, S. Auephanwiriyakul, Boundary detection in medical images using edge following algorithm based on intensity gradient and texture gradient features. IEEE Trans Biomed Eng. 2011, 58(3):567-73.

[53] R. Stolkin, et al. An EM/E-MRF algorithm for adaptive model based tracking in extremely poor visibility. Image and Vision Computing, 2008, 26(4): 480-495.

[54] P. N. Suganthan, Particle swarm optimizer with neighborhood operator, Proc. of the Congress on Evolutionary Computation. Piscataway, IEEE Service Center, 1999, pp: 1958-1962.

[55] J. Sun, B. Feng, W. B. Xu, Particle swarm optimization with particles having quantum behavior, Pro. of Congress on Evolutionary Computation.2004, pp:325-331.

[56] K. P. Wei, et al. An improved threshold selection algorithm based on particle swarm optimization for image segmentation. Natural Computation, 2007. ICNC 2007. Third International Conference on. Vol. 5. IEEE, 2007.

[57] J. Sun, X. J. Wu, W. Fang, and Y. R. Ding, et al., Multiple sequence alignment using the Hidden Markov Model trained by an improved quantum-behaved particle swarm optimization, Information Sciences, 2012, 182(1): 93-114.

[58] M. L. Xi, J. Sun and W. B. Xu, An Improved Quantum-Behaved Particle Swarm Optimization Algorithm with Weighted Mean Best Position, Applied Mathematics and Computation, 205, 2008, pp. 751-759.

[59] M. C. Yang, W. K. Moon, et al. Robust Texture Analysis Using Multi-Resolution Gray-Scale Invariant Features for Breast Sonographic Tumor Diagnosis, IEEE Trans. Med. Imaging, 2013, 32(12): 2262-2273.

[60] J. C. Yen, F. J. Chang, S. Chang, A new criterion for automatic multilevel thresholding, IEEE Trans on Image Processing, 1995, 4(3), pp: 370-377.

[61] E. Zahara, , S.-K. S. Fan, and D.-M. Tsai. Optimal multi-thresholding using a hybrid optimization approach. Pattern Recognition Letters, 2005, 26(8): 1082-1095.

[62] Y. J. Zhang , J. J. Gerbrands, Transition region determination based thresholding, Pattern Recognition Letter, 1991, 12(1), pp: 13-23.

[63] Y. Y. Zhang, M. Brady, and S. Smith. Segmentation of brain MR images through a hidden Markov random field model and the expectation-maximization algorithm. Medical Imaging, IEEE Transactions on, 2001, 20(1): 45-57.

[64] Y. L. Zheng, L. H. Ma, L. Y. Zhang, Empirical study of particle swarm optimizer with an increasing inertia weight. In: Proceedings of IEEE congress on evolutionary computation, Canbella, Australia, 2003, pp 221–226.

Yangyang Li received the B.S. and M.S. degrees in Computer Science and Technology from Xidian University, Xi'an, China, in 2001 and 2004 respectively, and the Ph.D. degree in Pattern Recognition and Intelligent System from Xidian University, Xi'an, China, in 2007.

She is currently an associate professor in the school of Electronic Engineering at Xidian University. Her current research interests include quantum-inspired evolutionary computation, artificial immune systems, and data mining.